Optical and electrical properties of indium tin oxide thin films sputter-deposited in working gas containing hydrogen without heat treatments

Suning Luo,[a,b] Koichi Okada,[a] Shigemi Kohiki,[a,]* Fuki Tsutsui,[a] Hirokazu Shimooka,[a] and Fumiya Shoji[c]

[a]*Department of Materials Science, Kyushu Institute of Technology, Kitakyushu 804-8550, Japan*
[b]*Liaoning Institute of Technology, China*
[c]*Kyushu Kyoritsu University, Kitakyushu 807-8585, Japan*

ABSTRACT

Polycrystalline thin films of indium tin oxide sputter-deposited in the working gas containing hydrogen of 0.3-1.5 % exhibited transmittance of ≥80 % for visible lights and blue-shift of ≥0.1 eV in the optical absorption energy. The film deposited in the gas containing hydrogen of 1 % demonstrated almost flat temperature-dependent resistivity and the lowest resistivity of $\approx 1.5\times10^{-4}$ Ωcm at room temperature. The carrier density showed an inverse V-shaped behavior with the maximum at the hydrogen concentration of 1 %. The mobility stayed at almost constant below the hydrogen concentration of 1 % and dropped rather rapidly above 1 %.

*Corresponding author. Tel.: +81-93-884-3300; Fax: +81-93-884-3310, E-mail address: kohiki@che.kyutech.ac.jp

1. Introduction

Thin films of transparent conducting oxides (TCOs) based on indium oxide (In_2O_3), tin oxide (SnO_2) and zinc oxide (ZnO) catch the attention of researchers in the fields of semiconductor and electronic materials [1-3]. Recently ZnO attracts great interests for its potential applicability in optical devices. On the other hand, indium tin oxide (ITO) has been the most widely used TCO in semiconductor and electronic device industry [4-6]. Sources of charge carriers in ITO with *n*-type conductivity are point defects such as doped Sn^{4+} ions substituted for In^{3+} ions at the cation sites and oxygen vacancy at the anion sites in the In_2O_3 crystal lattice. In_2O_3 crystallizes in the *C*-type rare-earth structure with space group of the *Ia*-3 [7]. The cubic unit cell contains 16 In_2O_3 formula units with fluorite-type unit cells accompanying systematic oxygen vacancies. From a consideration of electroneutrality, one Sn^{4+} ion and one oxygen vacancy generate one electron and two electrons in the crystal, respectively. Oxygen vacancy is expected to result in denser carriers of ITO especially at low temperatures than Sn^{4+} substitution. It is known that oxygen vacancy is predominant donor in undoped In_2O_3 [8,9].

Sputter-deposited TCO films demonstrate diverse electronic properties depending on the deposition conditions, i.e., partial pressure of oxygen, substrate temperature, deposition rate, and composition of target [10-12]. Addition of hydrogen is also effective to achieve a low resistivity for films of ZnO [13] and of ITO [14,15] deposited without substrate heating. It is believed that high-energy plasma in sputter-processes can substitute for both a high substrate temperature in the deposition and a post-deposition heating in air at 300 - 500 ^oC. It has been known that the post-deposition heating process oxidizes metallic components in the as-deposited film, and then lowers the resistivity [16,17]. In this work, we examined the optical and electrical properties of ITO films sputter deposited in plasma consisted of hydrogen and argon gases. We eliminated heat treatments such as the substrate heating in the deposition and the post-deposition heating in air to examine directly effects of hydrogen in working gas on the optical and electrical properties of the deposited ITO films.

2. Experimental

Films of ITO were deposited on alkali free glass substrates without substrate heating by low-pressure plasma sputtering of a sintered target (Kojundo Chemical, Japan) in the working gas containing hydrogen. The target consisted of In_2O_3 (95 wt %) and SnO_2 (5 wt %). Deuterium gas (99.99% purity) and argon gas (99.9999% purity) were introduced to deposition chamber of the base pressure $\approx 1\times10^{-7}$ Torr. Films were deposited at the hydrogen partial pressures of $\approx 1\times10^{-7}$ - 3.6×10^{-5} Torr. The gas pressure ratio of hydrogen to argon was in the range 0 - 3.6 %. While the films were deposited without substrate heating, the substrate temperature raised up to 250 ^{o}C by the plasma after 40 minutes from start of the deposition. By the deposition of 120 minutes, the film thickness reached to ≈200 nm, and the films were automatically heated at 250 ^{o}C. X-ray diffraction pattern of the films measured with a Rigaku CN2013 diffractometer using Cu $K\alpha$ radiation exhibited peaks ascribable to the In_2O_3 cubic crystal lattice (not shown). The films deposited without heat treatments were polycrystalline ITO.

3. Results and discussion

3.1. Optical properties

It is well known that the color of ITO bulk varies pale yellow to gray with degree of reduction. The films a, b, c, d, and e were deposited in the working gas containing hydrogen of 0, 0.3, 1, 1.5 and 3.6 %, respectively. The films a, b, c, and d were transparent for eye, and exhibited transmittance of over 80 % in the visible region, as shown in the lower panel of Fig. 1. The film e was grayish, and showed transmittance of ≈35 % for visible lights. The film e is considered to contain metallic components, and also to exhibit rather high resistivity unless adequately heated in air. In sputter-deposition of the ITO films in the gas containing hydrogen, In_2O_3 will decompose into In_2O_{3-x} (process I), and then the In_2O_{3-x} will further decompose into metallic In (process II). Thus, hydrogen is expected to remove oxygen from the plasma by forming H_2O and/or OH species in vapor phase, and then to result in ITO with an oxygen deficiency in solid phase. The transmittance of ≥80 % for the films deposited in the gas containing hydrogen of 0.3-1.5 % was brought about by the process I. The transmittance of ≈35 % for the film deposited in the gas containing hydrogen of 3.6 % was caused by the process II. Such decrease of the transmittance is considered as a result of an enlargement of reflection due to metallic In dispersed in the film.

Absorption coefficient α for the films b, c, and d shifted to the higher energy side than that for the film a, as shown in the upper panel of Fig. 1. The blue-shift of ≥0.1 eV at $\alpha = 0.45\times10^{5}$ cm^{-1} for the films deposited in the gas containing hydrogen can be attributed to the carrier density-sensitive Moss-Burstein shift [18]. Consequently, the films b, c, and d are expected to exhibit electric conductivity by a degenerate electron gas.

3.2. Electrical properties

As shown in Fig. 2, the films exhibited almost flat temperature dependence of resistivity as expected for degenerated semiconductors [19]. However, there was no linear relation between the resistivity and the hydrogen concentration in the gas. The film deposited in the gas containing hydrogen of 1 % exhibited the lowest resistivity (≈2.4×10^{-4} Ωcm at 275 K). The resistivity became larger for the films deposited in the gas containing hydrogen of 0.3, 0, 1.5, and 3.6 %. The resistivity of the films deposited in the gas containing hydrogen of 0 % and 3.6 % were ≈4.9×10^{-4} and ≈7.2×10^{-4} Ωcm at 275 K, respectively. The film deposited in the gas containing hydrogen of 3.6 % exhibited the highest resistivity as expected from the optical absorption spectra. The trend in resistivity suggests that charge carriers presented in the vicinity of the conduction band minimum do not necessarily mirror the hydrogen concentration in the gas.

As shown in the lower panel of Fig. 3, the resistivity at room temperature (RT) remained at almost constant (≈$1.5\text{-}3.5\times10^{-4}$ Ωcm) below the hydrogen concentration of 1.5 % in the gas, but further addition of hydrogen to 3.6 % caused apparent increase of the resistivity to ≈12×10^{-4} Ωcm. The cation reduction resulting in metallic-particles dispersed in the film became prominent in the optical and electrical behavior above the hydrogen concentration of more than 1.5 % in the gas.

The resistivity of the films can be partitioned into two terms of the carrier density and the mobility, as shown in the upper panel of Fig. 3. The carrier density indicated an inverse V-shaped behavior peaked around the hydrogen concentration of 1 % in the gas. The mobility stayed almost constant below the hydrogen concentration of 1 %, and fell down rapidly above

1%. The lattice defects resulting in mobile carriers of ITO are generally ionized, and they scatter carriers strongly [20-24]. Both a low carrier density and a high mobility for the films deposited in the gas of hydrogen below 1 % suggest that doped hydrogen resulted in oxygen defects in the crystal, and the oxygen defects compensated cation defects in the crystal and formed neutral defects. Judging from both a high carrier density and a low mobility for the films deposited in the gas of hydrogen above 1 %, hydrogen generated oxygen defects sufficient for prevailing over the neutral defect formation. The carrier transport with a high electron density and a low scattering achieved just at the hydrogen concentration of 1 % in the gas, and resulted in the lowest resistivity of ≈1.5×10^{-4} Ωcm at RT.

Hydrogen in the working gas influenced not only the optical and electrical properties but also surface morphology and microstructure of the films. Thin film analyses using scanning electron microscope and transmission electron microscope are now ongoing [25].

4. Summary

Polycrystalline ITO thin films deposited in the working gas containing hydrogen of 0.3-1.5 % showed the transmittance of ≥80 % in visible region and the resistivity of ≈$1.5\text{-}3.5\times10^{-4}$ Ωcm at RT. The blue-shift of ≥0.1 eV in the optical absorption and the almost flat temperature dependence of resistivity reflected a high carrier density at the bottom of the conduction band. The lowest resistivity of ≈1.5×10^{-4} Ωcm at RT was achieved by the deposition in the working gas containing hydrogen of 1 %.

References

[1] D. Ginley, C. Bright, *MRS Bulletin* **25**, 15 (2000).

[2] C. G. Granqvist, A. Hultaker, *Thin Solid Films* **411**, 1 (2002).

[3] S. Lany, A. Zunger, *Phys. Rev. Lett.* **98**, 045501 (2007).

[4] A. Salehi, *Thin Solid Films* **324**, 214 (1998).

[5] J. K. Sheu, Y. K. Su, G. C. Chi, M. J. Jou, C. M. Chang, *Appl. Phys. Lett.* **72**, 3317 (1998).

[6] B. Lewis, D. Paine, *MRS Bulletin* **25**, 22 (2000).

[7] M. Marezio, *Acta Crystallogr.* **20**, 723 (1966).

[8] J. H. W. Dewit, *J. Solid State Chem.* **8**, 142 (1973).

[9] J. H. W. Dewit, G. Vanunen, M. Lahey, *J. Phys. Chem. Solids* **38**, 819 (1977).

[10] H. Y. Chen, C. F. Qiu, M. Wong, H. S. Kwok, *IEEE Electron Device Lett.* **24**, 315 (2003).

[11] K. Zhang, F. Zhu, C. H. A. Huan, A. T. Wee, *J. Appl. Phys.* **86**, 974 (1999).

[12] R. X. Wang, D. Beling, A. B. Djurisic, S. Li, S. Fung, *Semicond. Sci. Technol.* **19**, 695 (2004).

[13] S. Kohiki, M. Nishitani, T. Wada, T. Hirao, *Appl. Phys. Lett.* **64**, 2876 (1994).

[14] S. Ishibashi, Y. Higuchi, Y. Ota, K. Nakamura, *J. Vac. Sci. Technol.* A**8**, 1399 (1990).

[15] S.N. Luo, A. Kono, N. Nouchi, F. Shoji, *J. Appl. Phys.* **100**, 113701 (2006).

[16] R.X. Wang, C. D. Beling, S. Fung, A. B. Djurisic, C. C. Ling, S. Li, *J. Appl. Phys.* **97**, 033504 (2005).

[17] R.X. Wang, C. D. Beling, S. Fung, A. B. Djurisic, C. Kwong, S. Li, *J. Phys. D: Appl. Phys.* **38**, 2000 (2005).

[18] I. Hamberg, C. G. Granqvist, *J. Appl. Phys.* **60**, R123 (1986).

[19] J. C. C. Fan, J. B. Goodenough, *J. Appl. Phys.* **48**, 3524 (1977).

[20] M. Chen, Z. L. Pei, X. Wang, Y. H. Yu, X. H. Liu, C. Sun, L. S.Wen, *J. Phys. D: Appl. Phys.* **33**, 2538 (2000).

[21] D. H. Zhang, H. L. Ma, *Appl. Phys. A* **62**, 487 (1996).

[22] M. Chen, Z. Pei, X. Wang, C. Sun, L. Wen, *Mater. Res. Soc. Symp. Proc.* **666**, F2.3/1 (2001).

[23] T. Minami, S. Suzuki, T. Miyata, *Mater. Res. Soc. Symp. Proc.* **666**, F1.3/1 (2001).

[24] A. S. Gilmore, A. Al-Kaoud, V. Kaydanov, T. R. Ohno, *Mater. Res. Soc. Symp. Proc.* **666**, F3.10/11 (2001).

[25] S.N. Luo, K. Okada, S. Kohiki, M. Mitome, unpublished (2008).

Figure captions

Fig. 1. Optical transmission spectra (lower panel) and absorption coefficient (upper panel) in ultraviolet-visible region measured by a JASCO V-550 spectrometer for the films deposited in the gas containing hydrogen of 0 (a), 0.3 (b), 1 (c), 1.5 (d), and 3.6 % (e).

Fig. 2. Temperature dependence of resistivity measured with conventional four probe method of the films deposited in the gas containing hydrogen of 0 (a), 1 (b) and 3.6 % (c). Platinum electrodes with a thickness of ca. 100 nm were made by a sputtering method on the films, and they were bonded by gold wires to the measurement system.

Fig. 3. Resistivity (lower panel), and carrier density and mobility (upper panel) of the films at RT versus hydrogen concentration in the working gas. The Hall effects for the films were measured with the van der Pauw method.

S.L fig.1

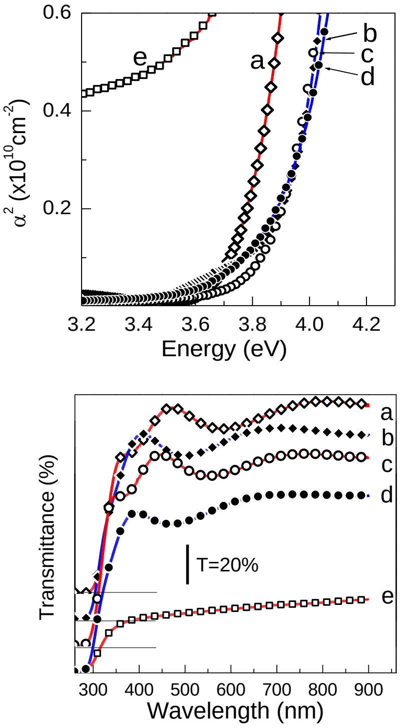
0.6
0.4
0.2
α^2 (x10^{10}cm^{-2})
e
a
b
c
d
3.2
3.4
3.6
3.8
4.0
4.2
Energy (eV)
Transmittance (%)
a
b
c
d
T=20%
e
300
400
500
600
700
800
900
Wavelength (nm)

S.L fig. 2

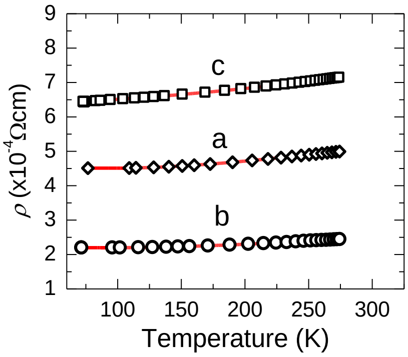

S.L fig. 3

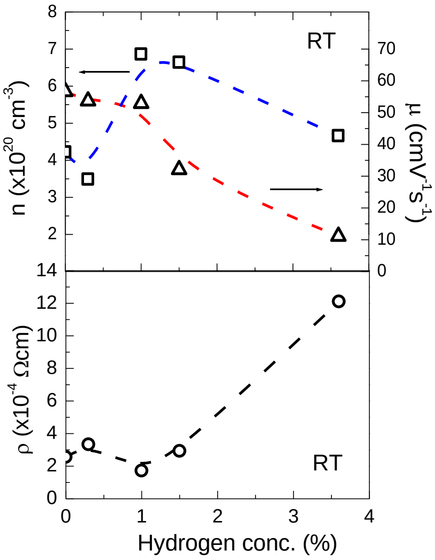
RT
n (x10^{20} cm^{-3})
μ (cmV^{-1}s^{-1})
8
7
6
5
4
3
2
70
60
50
40
30
20
10
0
14
12
10
8
6
4
2
0
ρ (x10^{-4} Ωcm)
RT
0
1
2
3
4
Hydrogen conc. (%)